Journal of
Alzheimer's Disease & Parkinsonism

Borgognon et al., J Alzheimers Dis Parkinsonism 2017, 7:5
DOI: 10.4172/2161-0460.1000383

Research Article OMICS International

Enhancement of Striatal Dopaminergic Function Following Autologous Neural Cell Ecosystems (ANCE) Transplantation in a Non-Human Primate Model of Parkinson's Disease

Simon Borgognon[1#], Jérôme Cottet[1#], Véronique Moret[1], Pauline Chatagny[1], Nathalie Ginovart[2], Cristian Antonescu[3], Jocelyne Bloch[4], Jean-François Brunet[5], Eric M Rouiller[1*] and Simon Badoud[1]

[1]Laboratory of Neurophysiology of Action and Hearing, Research cluster Neurosciences, Swiss Primate Competence Center for Research (SPCCR), Department of Medicine, University of Fribourg, Fribourg, Switzerland
[2]Department of Psychiatry, University of Geneva, Geneva, Switzerland
[3]Fribourg Cantonal Hospital (HFR), Nuclear Medicine Unit, Fribourg, Switzerland
[4]Department of Neurosurgery, Lausanne University Hospital (CHUV), Lausanne, Switzerland
[5]Cell Production Center (CPC), Lausanne University Hospital (CHUV), Lausanne, Switzerland
[#]Authors contributed equally

Abstract

Objective: Previous evidence was provided that parkinsonian monkeys exhibited significant though incomplete behavioral recovery following a cell therapy consisting of auto-transplantation of adult neural progenitor cells. The aim of the present study was to assess for the first time in this parkinsonian non-human primate model the striatal dopaminergic function, in parallel to further behavioral assessment. In other words, is the behavioral recovery associated to a reversal of dopaminergic function despite the auto-transplanted cells are not dopaminergic.

Methods: Striatal dopaminergic function and motor behavior (spontaneous motion activities) were monitored in adult parkinsonian macaques in relation to autologous neural cell ecosystem (ANCE) transplantation. In four MPTP intoxicated macaques, adult progenitor cells derived from cortical biopsies were re-implanted in the same animal after a phase of spontaneous functional recovery. The function of the striatal dopaminergic system was assessed using 18F-DOPA positron tomography imaging and the motor function was quantified.

Results: Two parkinsonian animals exhibited severe motor symptoms, which were moderate and transient in two other monkeys. 18F-DOPA striatal uptake decreased by 80% in three animals, consistent with losses of dopaminergic neurons in substantia nigra and reduced striatal density of dopaminergic projections. Six months after autologous transplantation, all animals improved their motor functions. This functional recovery was largely consistent with positron emission tomography results showing some recovery of 18F-DOPA striatal uptake toward baseline value following transplantation.

Conclusion: The present data confirm that symptoms are variable across individual parkinsonian monkeys and that autologous neural cell ecosystem transplantation indeed attenuates parkinsonian motor symptoms. Yet the present study provides for the first time evidence in favor of an increase in the striatal dopaminergic activity that correlates with motor recovery in this novel therapeutic approach, although the implanted cells are not dopaminergic.

Keywords: F-DOPA PET scan; MPTP; Macaque monkeys; Cell therapy; Motor behaviour; TH-immunocytochemistry

Introduction

Parkinson's disease (PD) is characterized by dopaminergic neuron loss in the substantia nigra (SN) pars compacta. The cardinal symptoms appear after 60 to 70% of neuronal loss within the SN and consist of akinesia/bradykinesia, rigidity and tremor at rest [1-6]. The correlation between the motor symptoms (specially bradykinesia) and a decrease of the dopaminergic striatal activity has been shown in PD patients by using positron emission tomography (PET) scans with [18F]-L-dihydroxyphenylalanine (18F-DOPA) [7]. Furthermore, in the non-human primate (NHP) 1-methyl-4-phenyl-1,2,3,6-tetrahydropyridine (MPTP)-induced model of PD, 18F-DOPA PET scan measure of presynaptic dopaminergic integrity is broadly used and gives valuable clues about the nigrostriatal state after MPTP intoxication [8,9]. Both in PD patients and NHP MPTP model, a low number of dopaminergic neurons in the SN is associated with a decrease in 18F-DOPA PET uptake in striatum [10,11].

Although widely studied since several decades, the biological mechanisms underlying PD's etiology remain largely unknown, making the development of efficient therapies a challenge. In spite of positive outcomes of deep brain stimulation and/or levodopa therapies, the progression of the pathology is neither stopped nor reversed [12-16].

The last two decades have seen the emergence of new hope based on promising results of cell therapies. This new approach represents an attractive alternative to conventional treatment and consists in the replacement of the depleted dopaminergic neurons using different cell sources [17]. Yet, although crucial steps have been achieved regarding the understanding of cell engraftment mechanisms, several issues remain to

***Corresponding author:** Eric M Rouiller, Laboratory of Neurophysiology of Action and Hearing, Research cluster Neurosciences, Swiss Primate Competence Center for Research (SPCCR), Department of Medicine, University of Fribourg, Fribourg, Switzerland, Tel: +41 26 300 86 09; E-mail: eric.rouiller@unifr.ch

Received September 26, 2017; **Accepted** October 05, 2017; **Published** October 12, 2017

Citation: Borgognon S, Cottet J, Moret V, Chatagny P, Ginovart N, et al. (2017) Enhancement of Striatal Dopaminergic Function Following Autologous Neural Cell Ecosystems (ANCE) Transplantation in a Non-Human Primate Model of Parkinson's Disease. J Alzheimers Dis Parkinsonism 7: 383. doi: 10.4172/2161-0460.1000383

be solved before considering large-scale therapeutic applications. The large amount of donor fetal tissues, immunosuppressive drugs and graft-induced side-effects are some of the limitations associated with the use of fetal midbrain tissues [18,19]. Moreover, embryonic stem cell engraftment raises the issue of tumor formation due to uncontrolled cellular proliferation and ethical controversies [20,21]. Recently, the induced pluripotent stem cell approach showed positive outcomes in NHP MPTP model but these positive results still need to be confirmed [22].

At the margin of those mainstream cell therapy approaches, Brunet et al. have developed an innovative method allowing the generation of long-term primocultures from human cortical tissues [23]. Similar results were then obtained from NHP cortical biopsies [24]. Further investigation revealed the presence of doublecortin-positive cells in in-vitro cell cultures [25]. Those cells need close interaction with astrocytes, building a niche necessary to their development. This association is referred as autologous neural cell ecosystems (ANCE). In a therapeutic perspective, ANCE have been implanted in symptomatic NHP MPTP model [26]. All the ANCE implanted animals, except one, exhibited a statistically significant reduction of PD symptoms, while the two other groups of monkeys (sham-grafted and killed-cell grafted) did not show any improvement. Interestingly, the implanted ANCE cells did not become tyrosine-hydroxylase (TH) positive cells. The positive behavioral effect of ANCE transplantation is thus most likely due to the release of neurotrophic factors [26,27].

As outlined in Table 1, the present study is the logical continuation and extent of two previous reports on the ANCE approach applied to MPTP monkeys [26,27]. Brunet et al. [27] and Bloch et al. [26] included in their ANCE studies control animals and the fate of the implanted cells was reported. Due to strict ethical guidelines restricting drastically the use of NHPs, controls were not repeated in the present study (Table 1). Furthermore, investigations on the fate of the implanted cells were not repeated either (Table 1). The aim of the present study was rather to focus on an original issue, by investigating nigro-striatal dopaminergic function with 18F-DOPA PET scans in four adult macaque monkeys subjected to MPTP lesion and ANCE transplantation. Moreover, in order to extend the behavioral dimension as compared to earlier reports [26,27], the four MPTP monkeys subjected to ANCE of the present study were enrolled in an assessment of spontaneous motion activities, using an image analyzer system performing an objective evaluation of the motor symptoms [28]. As emphasized above (ethical restrictions) and capitalizing on the already demonstrated efficacy of ANCE transplantation in a symptomatic PD monkey model including control animals ([26]; Table 1), all four macaques involved in the present study were subjected to a systemic MPTP lesion followed by ANCE transplantation.

Methodology

General survey of the experimental protocol

Globally, the present study comprised three main periods (Figure 1): the pre-lesion phase, the post-MPTP lesion phase and the ANCE post-transplantation phase. The pre-lesion phase spanned from spring 2010 to summer 2014 and encompassed training of the animals to different motor tasks (mainly manual dexterity, not reported in this present manuscript). The post-MPTP lesion phase consisted in the behavioral

	Monkey species	n=	Control monkeys #	PD symptoms	ANCE survival (%)	Quantitative behavior
Study 1 *	St-Kitt Green monkey	8	Yes	No	50.4 (+- 14.6) (at 4 months)	No
Study 2 **	St-Kitt Green monkey	9	Yes	Yes	27.1 (+- 6.7) (at 6 months)	Yes: Parkinsonian score (29 parameters)
Present study	Macaca fascicularis	4	No Not repeated	Yes	Not repeated &	Yes: Schneider scale and spontaneous motion activity

	ANCE cells migration	TH-immuno: Cell counts in *S. nigra*	GDNF-immuno	Striatal dopaminergic function assessed with PET (18F-DOPA)
Study 1*	Yes: contralateral hemisphere, corpus callosum	Yes	Yes: increase in ANCE monkeys	No
Study 2**	Not reported	Yes	No	No
Present study	Not repeated&	Yes	Not repeated &	Yes

* Brunet et al. [27]: asymptomatic monkeys (low dose MPTP treatment)
** Bloch et al. [26]: PD symptoms (higher MPTP doses)
# In study 1: Two intact controls, two MPTP controls without ANCE; In study 2: MPTP monkeys (n=2) who received no cell graft or killed-cell grafts.
& in the present study, possibly due to the advanced age of the animals, the histological tissue exhibited strong auto-fluorescence, preventing identification of the PKH67 re-implanted cells and therefore to repeat previous histological analyses (survival, migration, etc.)
Table 1: Overall survey of the long-term ANCE project on MPTP monkeys (3 consecutive studies).

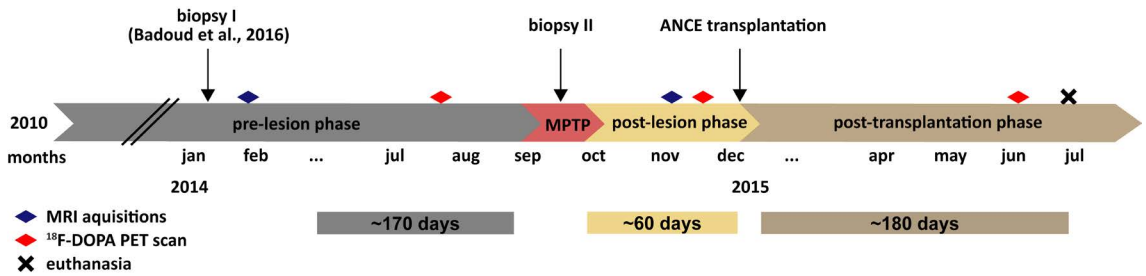

Figure 1: The time line illustrates the experimental protocol schedule. During the pre-lesion phase a first biopsy was performed in order to assess its potential impact on the behavioral tasks and to develop the good manufacturing practice (GMP) protocol [29]. The second biopsy, which provided the cellular material finally transplanted, was performed during the MPTP phase, thus better reflecting the clinical conditions of Parkinson's disease.

follow-up of the animals, during a period of eight weeks, to assess the impact of the MPTP lesion. Finally, the ANCE post-transplantation phase, that covered a period of six months, was dedicated to the monitoring of the animals in order to assess any potential effect of the treatment. As the treatment tested here is based on in vitro culture of cortical tissues [23,24,26,27], two biopsies were obtained for each animal (one during the pre-lesion phase [29] and one during the MPTP protocol).

Within each experimental period, the function of the dopaminergic system was assessed by 18F-DOPA PET scans. Moreover, structural magnetic resonance imaging (MRI) data were acquired to identify the stereotaxic coordinates targeted in the transplantation surgeries. At the end of the protocol, the animals were euthanized for histological purposes (Figure 1). Data were transferred into Microsoft Excel files for compilation and analysis; the graphical representations and the statistical analysis were performed in MATLAB (R2015b).

Animals

Four female adult macaques (*Macaca fascicularis*) ranging from 6 to 10 years old and weighing between 3 and 5 kg at the beginning of the pre-lesion phase, were involved in this study. All four animals were housed in the animal facility of the University of Fribourg in an enriched indoor room of 45 m^3 (for a group of 2-5 monkeys, as requested by the Swiss law on animal protection), with supplementary access to an outdoor space. Animals could interact with each other and were free to move (http://www.unifr.ch/spccr/about/housing). They had free-access to water and were not-food deprived. Their identities were Mk-LL, Mk-LY, Mk-MY and Mk-MI. The entire experiment protocol was in accordance with the law on animal protection and accepted by the Federal and local veterinary authorities (authorization numbers 2012_01E_FR and 2012_01-FR).

Schneider MPTP scale

All four animals' behaviors were closely monitored using the Schneider scale [30]. This scale encompasses eight items rated from 0 (absent) to 3 (severe) that allow assessing the time-course of motor symptoms (upper limb movement, lower limb movement, ability to manipulate food, range of arm movement, bradykinesia/akinesia, hyperkinesia, tremor and dystonia). The behavioral evaluation was performed on a regular basis by the same experimenter in the animal housing facility by periods of about 20 min.

Spontaneous motion activity

Every day, animals were individually placed in a cage (52.5 cm × 115 cm × 82 cm) during 40 min. The first 10 min were aimed to habituate monkeys to the environment. During the next 30 min, spontaneous motion activity was assessed, corresponding to free will locomotor and other motor activities (free behaving), using the VigiePrimate® image analyzer system (View Point, Lyon, France). Different thresholds defined freezing, middle and burst activities (middle activity threshold at 500 and burst activity threshold at 2000 pixels change per seconds). Moreover, the system allowed tracking the traveled distance by following the center of mass of the animals. Statistical analyses (Wilcoxon rank sum test) compared each of the three experimental phases (pre-lesion, post-MPTP lesion and/or post-transplantation) in each animal. Data included in the pre-lesion phase were collected starting 6 months before the MPTP lesion protocol. The post-MPTP lesion phase encompassed only the data collected during the month (30 days) preceding ANCE transplantation. Data for the post-transplantation phase were collected during a period of 3 months before euthanasia. Differences in spontaneous motion activity were considered as statistically significant when the p-value was smaller than 0.05 ($p \leq 0.05$).

PET image acquisitions

PET scans with 18F-DOPA (Radiopharmazie, Klinik für Nuklearmedizin, Zürich, Switzerland) were conducted for each animal during each experimental phase. Animals received one hour before the 18F-DOPA injection, 50 mg *per os* of Carbidopa (Pharmacie internationale Golaz, Lausanne, Switzerland). The detailed anesthetic protocol during the acquisition as well as the structural magnetic resonance imaging protocol has been reported in our previous behavioral article related to the first biopsy [29]. Animals, in pronation position, were introduced into the scanner (Philips Ingenuity TF). First, a computer tomography (CT) acquisition was performed. Then, 18F-DOPA (about 125 MBq) was injected intravenously. Immediately after the injection, the PET data were acquired for 90 min in 28 frames of increasing duration from 30 s to 5 min.

18F-DOPA PET scans post-processing

Analysis of 18F-DOPA scans was done using the dedicated software PMOD V3.605 (PMOD Technologies Ltd., Zürich, Switzerland). First, native images were converted from DICOM format to NIfTI format. For the purpose of co-registration, summation PET images were generated over the 10-90-minutes of dynamic data and co-registered, using the CT scan, onto the T1-weighted MRI images using a six-rigid-body algorithm. The resulting transformation matrix was then applied to the PET dynamic images. Regions of interest (ROIs) for the left/right putamen, left/right caudate nuclei, and occipital cortex were then manually outlined on the MRI images and transferred onto the corresponding co-registered PET images. ROIs were manually adjusted on functional images in order to compensate for small miss-registration errors. Bilateral ROIs were pooled to obtain the average radioactivity concentration in the ROI. Regional radioactivity was determined for each frame, corrected for decay and plotted versus time to obtain times activity curves (TACs).

The influx rate constant, Ki (min^{-1}), for 18F-DOPA uptake in caudate and putamen was calculated (Table 2) using the Patlak multiple-time graphical analysis and the occipital cortex, a region with poor dopaminergic innervation [31,32], as reference region to estimate free and non-specific binding of the radiotracer in the brain [33]. For each animal, voxel-wise parametric maps of Ki were also generated using the Patlak approach and the occipital cortex as reference region as implemented in PMOD V3.605.

MPTP lesion

The present lesion protocol was adapted according to Mounayar et al. [34]. It consisted in series of daily intramuscular MPTP (Sigma-Aldrich Co; 0.5 mg/kg, dissolved in saline solution) injections, separated by break periods. The total amount of MPTP injected varied from 6.25 mg/kg (Mk-LY, Mk-LL and Mk-MY) to 7.75 mg/kg (Mk-

	Mk-LY	Mk-LL	Mk-MY	Mk-MI
Pre-lesion	0.00735	0.00787	0.00819	0.00857
Post-lesion	0.00610	0.00124	0.00151	0.00178
Post- transplantation	0.00739	0.00220	0.00326	0.00270

The table sums up the ^{18}F-DOPA PET scan striatal influx constant (Ki) values for all animals during each experimental phase

Table 2: ^{18}F-DOPA PET scan influx constant (Ki).

MI). During the last week, and according to the symptoms exhibited by each individual animal, the decision was taken to adjust or not the amount of MPTP injected.

Cortical biopsies

Two cortical biopsies were obtained from each animal's dorsolateral prefrontal cortex. The aim of the first biopsy, which was performed nine months prior to the MPTP lesion, was to assess its possible impact on the motor task performance and to refine the cell culture procedure for production under GMP (good manufacturing practices) rules in module Isocell Pro 1.8 (Euroclone) conducted at the CHUV (cell production center (CPC), CHUV, Epalinges, Switzerland) [29]. The second biopsy was performed during the MPTP phase to be closer to the clinical situation. These new GMP productions generated the ANCE, which had to be subsequently re-implanted in the MPTP-treated animals. All surgical procedures for biopsy are available in details in our previous study [29]. The cortical biopsies, limited in volume and spatially restricted to the prefrontal cortex, did not have significant impact on motor performance itself (scores) in the various behavioral tasks used in the laboratory, as previously reported [29,35].

Cell cultures and preparation for transplantation

Once the biopsies performed, the cortical samples were immediately processed to be put into culture conditions, as previously reported [24,26,27,36,37]. However, as a further development with respect to our previous studies, the present culture protocol was conducted according to GMP (good manufacture practice) standards in a Swissmedic accredited facility. Prior to implantations, the cells were labeled with PKH67 (MINI67; Sigma-Aldrich), a fluorescent dye that irreversibly binds to the cell membrane.

Cell transplantation

For each animal, two implantations sites in the putamen and one in caudate nucleus per hemisphere (six total implantation sites per animal) were determined based on T1-weighted MRI scan at post-MPTP lesion phase, and then compared with the Paxinos atlas of the macaque brain [38]. Transplantation surgeries followed the same surgical procedures as described in our previous study [29]. However, craniotomy was performed bilaterally in order to have access to stereotaxic coordinates of implantation sites. Implantation sites were reached vertically with a Hamilton microsyringe (100 µl, 22 G). Once the site was reached, a total volume of 10 µl culture medium (corresponding to approximately 300'000 cells) was automatically injected (2 µl/min during 5 min for each site) using a nano-injector (Stoelting, Wood Dale, IL, USA). After each injection, the needle was slowly withdrawn in order to avoid a suction effect that would have impacted on the position of the grafts. Once the six sites were implanted, the bone flap was put back in place; the muscles and skin were sutured as previously described [29].

Euthanasia

Animals were euthanized about six months after ANCE transplantation. For this purpose, the animals were first sedated with ketamine (10 mg/kg, i.m.) and then injected with a lethal dose of sodium pento-barbital (Esconarkon®; Streuli; 60 mg/kg; i.v.). Once the animals were deeply anesthetized, a trans-cardiac perfusion was initiated with 400 ml, 0.9% NaCl. The following solutions were successively perfused in order to fix and preserve brain tissues: 3 l of 4% paraformaldehyde (PFA) in 0.1 M phosphate buffer (pH 7.6) and 3 times 2 l of sucrose solutions of increasing concentrations (10%, 20%, 30%). Brains were then extracted and dissected before being placed for about ten days in a 30% sucrose solution. The brains were cut into ten series of 50 µm thick sections using a cryostat (HM560, MICROM, Volketswil, Switzerland). The series were then placed in a cryoprotective buffer (50 mM phosphate buffer, 25% glycerol, 35% ethylene glycol) at -20°C.

Histology

Staining of the TH-positive cells in the substantia nigra was done following a standard immunohistochemistry protocol. Histological sections were protected from light and incubated overnight, at room temperature, with the anti-TH antibodies (AB152, Merck-Millipore, 1:1000) in PBS, triton 0.3% and BSA (bovine serum albumin) 0.25%. In parallel, the second antibody conjugated to horseradish peroxidase (HRP) (AB97155, Abcam, 1:400) was incubated (overnight, 4°C) in PBS with a half monkey brain slice (not belonging to the present study) in order to remove the unspecifically bound antibodies. Incubation of the second antibody was done for 2 hours in PBS at room temperature. The revelation step consisted in incubating the brain sections with 3,3'-diaminobenzidine (DAB, D-5905, Sigma-Aldrich) in PBS with concentrated H_2O_2 during 30 min. Finally, the brain sections were mounted on microscopic slide and covered with quick-hardening mounting medium (Eukitt, 3989, Sigma-Aldrich).

The same immunohistochemical protocol was applied for visualizing the fluorescence density of TH-labeled axonal terminals in striatum. However, the second antibody used was conjugated with an infrared dye (611-145-122, Bioconcept, 1:500) and the step with DAB was omitted.

TH-positive cells charting analysis and photographic acquisitions were performed using a conventional light microscope Olympus BX40 (camera, MBF bioscience, Q imaging, color 12 bit) and the Neurolucida software (version 11.0). The total number of TH-positive neurons was reported for each brain section (a total of 8 brain sections per animals covering the entire substantia nigra). Photographic acquisitions of the infrared fluorescence density were performed using the Odyssey software (LI-COR bioscience, version 1.2, 2003). Subsequently, the fluorescence density was analyzed for each brain section (6 sections in total covering the entire striatum) with the Fiji software (ImageJ, version 2.0.0). A circle region was delineated in the striatum and in a reference region in the cerebral cortex. The fluorescence intensity density (IntDen) given by the software was reported. The final striatal fluorescence density value was obtained for each brain section by dividing the IntDen of the striatum with the reference cortical IntDen. Differences were considered as statistically significant (Wilcoxon rank sum test) when the p-value was smaller than 0.05 ($p \leq 0.05$). Note that three additional macaque monkeys (Mk-EN, Mk-GI and Mk-SA; not subjected to MPTP intoxication and derived from previous studies) were used as control animals (healthy control) in the histological procedures and for comparison of the TH-immunostaining with the 4 MPTP monkeys.

Conventional histological analysis was performed with the same light microscope on a series of Nissl stained sections of the brain to check the location of the ANCE transplantation sites (one in caudate nucleus and two in the putamen in each hemisphere). Similarly, another series of sections was analyzed for fluorescence in order to detect the presence and spatial distribution of the transplanted cells labeled with the fluorescent vital marker PKH67.

Statistical Analyses

For statistical analysis of 18F-DOPA data, a global statistical approach (random intercept linear mixed-effects model) was

performed. The Ki were considered as the response variable, the experimental phases as the fixed effects, whereas the identities of the animal as random effects (Table 3). The behavioral and histological data were analyzed using the non-parametric Wilcoxon test (Table 4).

Results

Schneider MPTP scale

All four MPTP animals progressively exhibited parkinsonian motor symptoms during the course of the MPTP injection protocol (Figure 2). In Mk-LY and Mk-LL, the motor symptoms emerged at the middle of the MPTP protocol and then slowly and progressively decreased starting two weeks after the last MPTP injection, reaching a plateau of modest Schneider score of 1-2. In Mk-MY, parkinsonian motor symptoms progressively appeared during the MPTP lesion protocol and remained stably elevated during several months after the last MPTP injection, before decreasing also to a modest score. Mk-MI showed nearly no motor symptoms during the MPTP protocol itself; however, few days after the last MPTP injection, severe motor symptoms exponentially emerged, remaining stable and deleterious for several months (Movie 1; Figure 2). In the three monkeys with a modest Schneider score several months post-MPTP lesion, the ANCE transplantation was followed within a few weeks by a final decrease of the Schneider score to zero, reflecting a normal motor function. In the monkey with severe motor symptoms (Mk-MI), the Schneider scale remained high (score 8-12) as long as a few weeks after ANCE transplantation, before a significant and quick decrease took place, stabilizing at low level (score of 2; Figure 2). In all monkeys, the Schneider score exhibited a fairly large day-to-day variability in terms of qualitative symptoms severity.

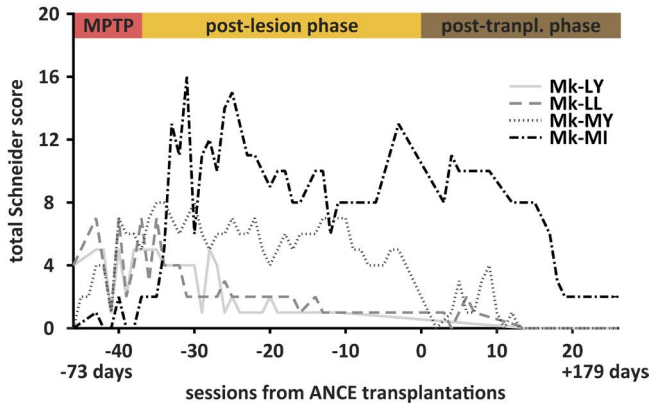

Figure 2: The graph plots a semi-quantitative assessment of the motor symptoms during and after the MPTP lesion protocol and after the ANCE transplantation, using the Schneider rating scale [30]. The higher the score, the worse were the parkinsonian symptoms. Along the abscissa, time corresponding to daily sessions in which the rating scale was established. The extremities of the abscissa correspond to time points of -73 and 179 days with respect to ANCE transplantation (day 0).

	Value	Std. error	DF	t-value	p-value
Intercept	0.007999	0.000837	9	9.553	5.2249e-06
Lesion	-0.005337	0.000980	9	-5.445	0.000408
Transplantation	-0.004105	0.000980	9	-4.187	0.002348

The table sums up the results of the random intercept linear mixed-effects model. The Ki values were considered as the response variables, the identities of the animals as random effects, whereas the experimental phases (pre-lesion, post-lesion and post-transplantation) as fixed effects

Table 3: Random intercept linear mixed-effects model.

	Mk-LY	Mk-LL	Mk-MY	Mk-MI
Pre-lesion vs. Post-lesion	4.34 e-05	1.10 e-09	2.27 e-10	2.27 e-10
Pre-lesion vs. Post-transplantation	0.019085	7.67 e-12	6.70 e-14	1.08 e-13
Post-lesion vs. Post-transplantation	0.255116	0.022249	1.20 e-07	5.31 e-08

p-values of the traveled distance (Figure 3B)

	Mk-LY	Mk-LL	Mk-MY	Mk-MI
Pre-lesion vs. Post-lesion	0.000216	1.32 e-09	2.27 e-10	1.52 e-09
Pre-lesion vs. Post-transplantation	0.052509	3.92 e-13	1.78 e-13	9.62 e-13
Post-lesion vs. Post-transplantation	0.128982	0.028879	6.52 e-07	2.55 e-07

p-values of the striatal fluorescence activity (Figure 4B)

EN vs. GI	0.1320						
EN vs. LY	0.0022	**GI vs LY**	0.0152	**LY vs LL**	0.0411	**LL vs MY**	0.2403
EN vs. LL	0.0022	**GI vs LL**	0.0043	**LY vs MY**	0.0260	**LL vs MI**	0.4848
EN vs. MY	0.0022	**GI vs MY**	0.0022	**LY vs MI**	0.0087	**MY vs MI**	0.0931
EN vs. MI	0.0022	**GI vs MI**	0.0022				

The table sums up the different p-values obtained with the Wilcoxon rank sum test for the time spent in freezing activity (Figure 3A), the traveled distance (Figure 3B) and the striatal fluorescence activity (Figure 4B). In the bottom panel, each monkeys' ID is given by the last 2 letters only (e.g. LY instead of Mk-LY)

Table 4: p-values of the time spent in freezing activity (Figure 3A).

The specific case of Mk-MI with severe motor symptoms after the MPTP treatment is of particular interest (Movie 1). As compared to the normal behavior, 4 days after the last MPTP injection, there was strong postural instability, bradykinesia, tremor and low speed motion in the detention room, although the animal could still feed by herself. The same symptoms persisted three weeks later. In sharp contrast, three months after ANCE transplantation, Mk-MI surprisingly recovered most motor functions, regaining nearly normal motor control ability (Movie 1).

Spontaneous motion activity

All four animals exhibited significant changes of their spontaneous motion activity patterns following MPTP lesioning. There was a significant increase of the freezing activity in all four animals post-MPTP lesion ($p \leq 0.001$; see Table 4 for for exact p-values), though more dramatic in Mk-MY and Mk-MI than in Mk-LY and Mk-LL (Figure 3A). After the ANCE transplantation, the freezing activity was reversed to some extent in all monkeys, although the decrease was not statistically significant in Mk-LY, which however displayed the least increase of freezing activity post-MPTP lesion. In the other three monkeys (Figure 3A), the reversal of freezing activity after ANCE transplantation was statistically significant as compared to the post-MPTP lesion period (Table 4). Spontaneous motion activity as observed in the three phases is illustrated for Mk-MI in (Movie 2), illustrating the dramatic loss of free motion as a result of MPTP intoxication (nearly 100% of freezing activity), followed by limited, though significant, re-appearance of middle motion activity. Consistent data were observed when considering another free motion parameter, namely the distance travelled by the monkey during the 30 minutes of the session (Figure 3B). The traveled distance decreased after MPTP lesion and then re-augmented after ANCE transplantation; again, there was a statistically significant effect observed after ANCE transplantation as compared to the post-MPTP lesion phase in the same 3 out of 4 monkeys (Table 4).

The same two behavioral parameters, freezing activity and traveled distance, were plotted as a function of time during the entire experimental protocol in the two monkeys exhibiting the most severe symptoms (Figures 3C and 3D): Mk-MI and Mk-MY). In both animals, the MPTP intoxication produced a dramatic increase of time spent in freezing activity and decrease of travelled distance. Interestingly, these

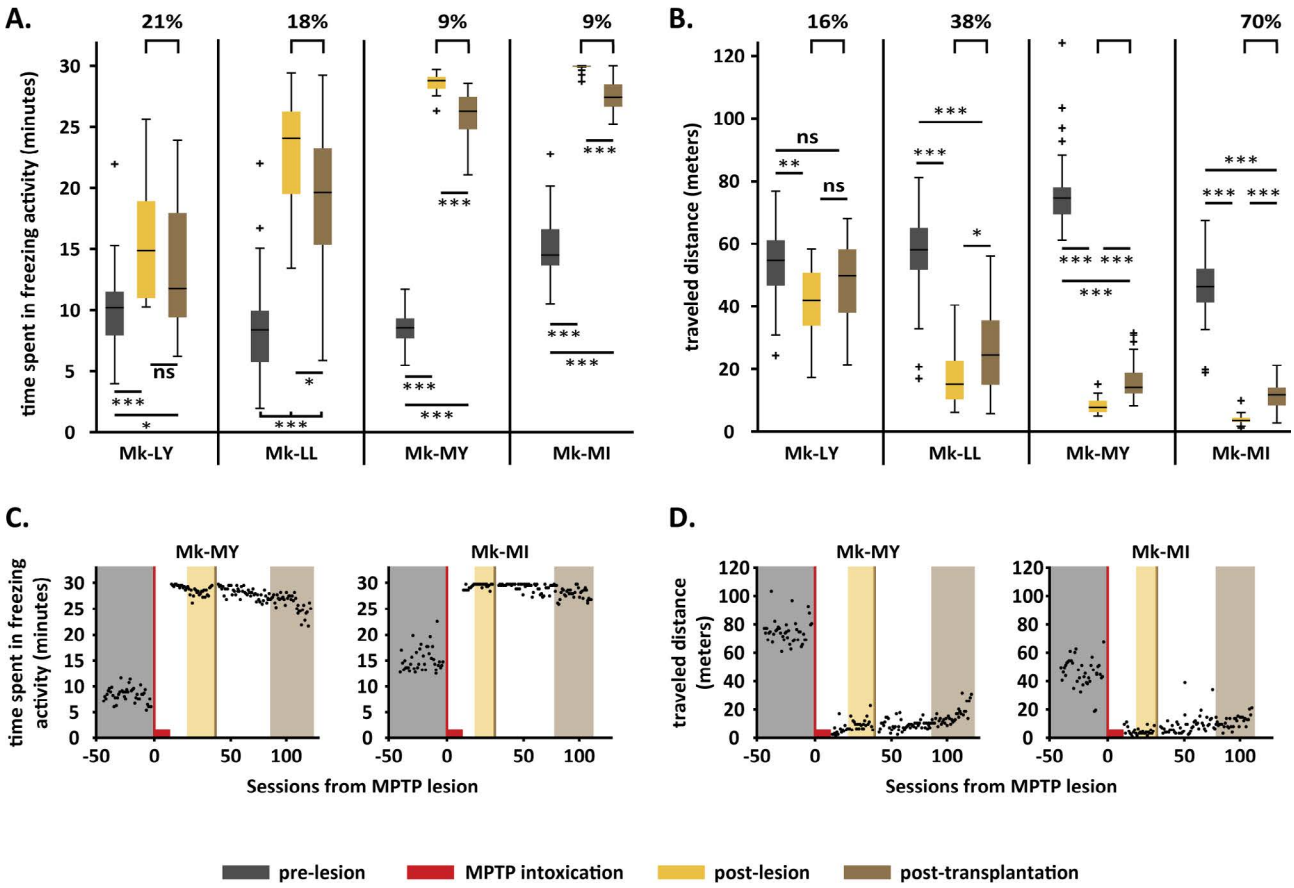

Figure 3: On top, the Box and whisker plots show the spontaneous motion activities of the four animals. (A) The time spent in freezing activity (when the animal was almost not moving) of the animals during a recording session of 30 min. All four animals exhibited an increase of the time spent in freezing activity after the MPTP lesion followed by decreases after the ANCE transplantation. (B) The travelled distance (in meters) during the recording session of 30 min. The percentages on top of each plots for each animal is the extent of recovery, calculated by comparing the median values post-MPTP lesion and post-ANCE transplantation (% of change of the post-lesion median value). The Wilcoxon rank sum test was applied for the statistical test. Statistically differences are indicated with: * for $p \leq 0.05$, ** for $p \leq 0.01$, *** for $p \leq 0.001$. "ns" is for statistically non-significant ($p>0.05$). See Table 4 for exact p-values.

On bottom (panels C and D), the same two behavioral parameters (freezing activity and travelled distance) are plotted as a function of time during the entire protocol, represented along the abscissa by the individual behavioral sessions (one data point for each daily session). Day 0 along the abscissa corresponds to the onset of MPTP intoxication, which lasted about 6 weeks (red rectangles). Negative session numbers corresponds to the pre-lesion period and positive ones to the post-lesion/post-transplantation period. The data are illustrated for the 2 monkeys in which the MPTP intoxication generated the most severe symptoms (Mk-MY and Mk-MI: see panels A and B).The color code is the same as in panels A and B in order to distinguish the pre-lesion, post-lesion and the post-transplantation time windows during which the behavioral data were collected and represented in the form of box plots in panels A and B.

two motor parameters remained largely stable during the whole post-lesion period before transplantation (about 2.5 months), indicating that there is no substantial spontaneous recovery. Following the ANCE transplantation (brown vertical lines in Figures 3C and 3D), there was a progressive reversal of the freezing activity and travelled distance, corresponding to the onset of a functional recovery, most likely related to the ANCE therapy. If one would have prolonged the period of post-transplantation observation, it is likely that the function recovery would continue with more decrease of time spent in freezing activity and increase of travelled distance. The extent of recovery observed here up to 120 days post-MPTP intoxication is already statistically significant as shown in panels A and B of Figure 3.

18F-DOPA PET imaging

During the pre-lesion phase, all four animals exhibited comparable Ki values, ranging from 0.00735 to 0.00857 for Mk-LY and Mk-MI, respectively (Table 2). About seven weeks after the last MPTP injection, a second PET acquisition was performed in each animal. Three out of four monkeys exhibited a dramatic decrease of the striatal uptake of 18F-DOPA, corresponding to about 80% loss as compared to pre-lesion values (Table 2 and Figure 4A). In Mk-LY, the decrease of the striatal uptake of 18F-DOPA was less prominent (-17%). The lesion impacted the striatum in a relatively global manner with minimal left/right asymmetry (data not shown). About six months after ANCE transplantation, as derived from a third PET acquisition, there was an unexpected re-increase of the PET signal in all four animals (Table 2 and Figure 4A), ranging from 11 to 21% across the 4 monkeys. Globally, statistical analyses revealed significant differences between the three experimental phases regarding the striatal Ki values ($p<0.01$; random intercept linear mixed-effects model) (Table 3).

Histology

As shown in Figure 4B, the striatal fluorescence density of TH-labeled axonal terminal fields was strong (ranging from 2 to 3.5) in two healthy

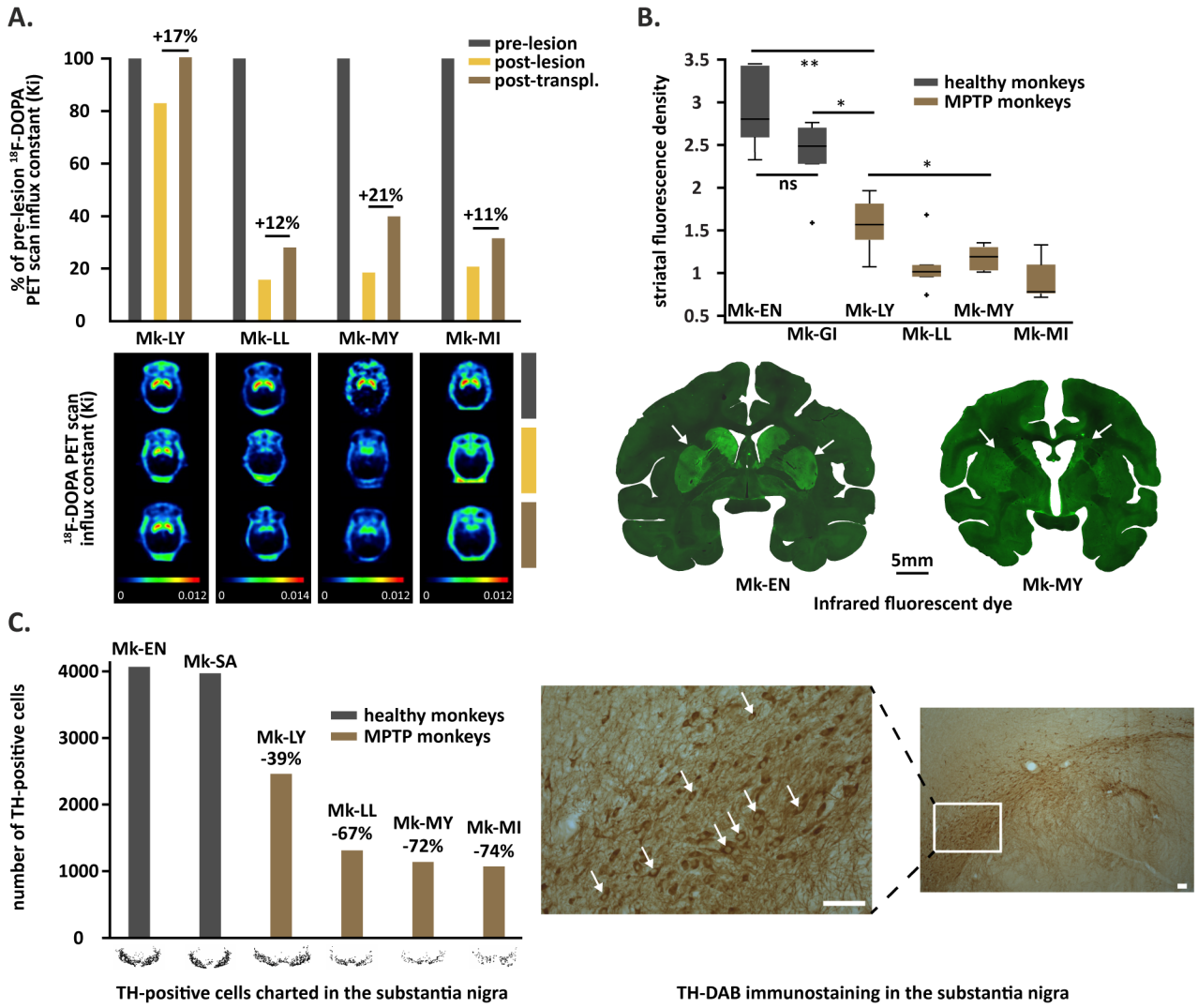

Figure 4: Dopaminergic state of the animals, as reflected by several readouts. (A) The influx constant (Ki) of 18F-DOPA is expressed as percentage of the baseline pre-lesion Ki value. After the MPTP lesion, all four animals showed a dramatic decrease of the striatal uptake of the 18F-DOPA (>80%) except Mk-LY (-17%). Those decreases were followed by uptake increases in all animals after ANCE transplantation. The bottom panel shows parametric maps of 18F-DOPA Ki in a horizontal plane for the 3 experimental phases in each animal. The colors represent the level of the 18F-DOPA uptake rate. The red color corresponds to a strong uptake rate, whereas the blue color to a weak uptake rate. (B) The striatal fluorescence density of the TH-labeled axonal terminals was strong in the 2 control, non-lesioned animals (Mk-EN and Mk-GI), whereas the 3 animals (Mk-LL, Mk-MY and Mk-MI) with a 80% loss of 18F-DOPA uptake exhibited much less fluorescent activity. In Mk-LY, the TH fluorescent density was intermediate. The Wilcoxon rank sum test was applied for the statistical test. Statistically differences are indicated with: * for $p \leq 0.05$, ** for $p \leq 0.01$, *** for $p \leq 0.001$. "ns" is for statistically non-significant ($p>0.05$). See Table 4 for exact p-values. The bottom panel exhibits a histological section of a healthy animal (Mk-EN) with a strong striatal TH fluorescent density (white arrows) and a MPTP animal (Mk-MY) with almost no TH fluorescence density (white arrows). (C) The average number of TH-positive neurons in the substantia nigra was 4016.5 in the 2 healthy of animals (Mk-EN and Mk-SA). Mk-LY showed about 40% less number of TH-positive neurons, whereas in the 3 other animals (Mk-LL, Mk-MY and Mk-MI), a decrease of about 70% of TH-positive neurons was observed. The right panel shows few examples of TH positive neurons in the substantia nigra in Mk-EN (white arrows). Scale bar=100 µm.

animals (control monkeys Mk-EN and Mk-GI), whereas the 3 MPTP-treated animals (Mk-LL, Mk-MY and Mk-MI), who showed about 80% loss of 18F-DOPA uptake, also exhibited much less fluorescent TH activity, a decrease which was statistically significant as compared to the 2 control animals ($p<0.01$). In Mk-LY, the striatal TH fluorescence density was intermediate, but still significantly lower than in control animals ($p<0.05$). Mk-LY showed a higher striatal TH fluorescence density than the other 3 MPTP-treated animals ($p<0.05$) (Figure 4B and Table 4 for exact p-values). Finally, the average number of charted TH-positive neurons in the substantia nigra was 4016.5 in 2 control animals (Mk-EN and Mk-SA). Mk-LY showed about 40% less TH-positive neurons in the substantia nigra whereas, in the other 3 MPTP animals (Mk-LL, Mk-MY and Mk-MI), the decrease was even larger (about 70%; Figures 4C and 4D).

The observation at low magnification (12.5x) of Nissl stained sections of the striatum confirmed that the ANCE transplantations were indeed placed in the targeted caudate and putamen nuclei in all 4 monkeys. Moreover, confirming previous ANCE transplantation trials in monkeys [26,27,37], there was no histological sign of tumor formation or teratoma. Finally, multiple PKH67 labeled cells were detected, exhibiting the same morphology as previously reported [26,27,37]. As expected, they were located around the implantation tracts but also at more remote zones of the striatum.

Discussion

Evidence that ANCE transplantation can significantly enhance functional recovery from parkinsonian motor deficits in MPTP-lesioned non-human primates (St.-Kitts monkeys) has been provided in earlier reports [26,27]. For this reason (as also outlined in Table 1), and due to logistic, legal and ethical limitations in the number of monkeys that can be enrolled in experiments in Switzerland, the present study did not include control animals, namely monkeys subjected to MPTP intoxication without ANCE transplantation (or sham transplantation). The goal here was instead to extend those previous reports [26,27] to an original longitudinal monitoring of the dopaminergic function with 18F-DOPA PET in parallel to the ANCE transplantation protocol conducted in the 4 monkeys enrolled in the present study. In addition, extensive behavioral data have been collected in these 4 monkeys, focused here on a clinical scoring of motor symptoms [30] and on spontaneous motion activity [28], for correlation with 18F-DOPA PET data (manual dexterity behavioral data will be reported elsewhere).

To summarize and interpret the PET data, the pre-lesion scans showed comparable striatal 18F-DOPA uptake values in the four monkeys, with Ki values ranging from 0.0073 (Mk-LY) to 0.0085 (Mk-MI), in line with previous reports (range 0.007 to 0.011 [9,11,39-41]). As expected, the post-MPTP lesion scans revealed clearly diminished striatal 18F-DOPA uptakes in all four animals, as well as large inter-individual variability (Table 2 and Figure 4A: three monkeys showed a decrease of about 80% whereas the fourth monkey exhibited a decrease of 17% only). Surprisingly, and this is an original observation to our knowledge, the post ANCE transplantation PET scan data in all four monkeys showed a re-increase of the striatal Ki values, ranging from 11% to 21% as compared to the post-MPTP lesion scan. This increase was statistically significant ($p<0.01$; Table 3), although the transplanted ANCE neural progenitor cells did not generate dopaminergic neurons, as it was observed that only very few transplanted cells were co-labelled with PKH67 (vital marker of the implanted cells) and TH in a similar MPTP model [26,27]. Several studies have assessed the evolution of the dopaminergic function in MPTP non-human primate models following offset of the MPTP intoxications [30,40,42]. None of them reported such a re-increase of striatal 18F-DOPA uptake after the last MPTP injection. In particular, Melega et al. conducted a longitudinal study of 18F-DOPA PET uptake at different time-points [40] and reported either stable striatal Ki or progressive decrease of the 18F-DOPA uptake over a period of one year post-MPTP intoxication. In absence of production of new dopaminergic neurons derived from the implanted ANCE cells, the significant re-increase of striatal 18F-DOPA uptake may be due to an indirect effect of the transplant, possibly via growth factors (see below), promoting sprouting of the nigrostriatal axons which survived the MPTP intoxication [34,43]. One may speculate that such sprouting of residual dopaminergic projection contributes to functional recovery, in cooperation with non-dopaminergic compensatory mechanisms [44,45]. The observation in monkey Mk-LY of a modest decrease of striatal 18F-DOPA uptake post-MPTP lesion (17%) may possibly be interpreted as a resistance to MPTP [46], at least to some extent.

On a behavioral point of view, all four animals were differently affected by the MPTP lesion (Figure 2; based on the semi-quantitative Schneider score), confirming the large inter-individual variability previously reported in the literature and representing an obvious limitation of the non-human primate MPTP model [34,46-48]. Such observed inter-individual variability places the present experimental model within the standards in the field (animal PD models). Mk-LY and Mk-LL almost fully recovered few days after the last MPTP injection while the two others (Mk-MY and Mk-MI) exhibited more severe and stable motor symptoms. Yet, more quantitative and objective assessments, for instance based on the high sensitivity of the video analyzer system used to quantify the spontaneous motion activity of the animals (VigiePrimate®), enabled to detect more subtle but still significant changes induced by the MPTP lesion [28,34,49,50], even in apparently asymptomatic monkeys such as Mk-LY and Mk-LL (Figure 3): in all four animals, there was a clear increase of the time spent in the freezing state and a decrease of the average travelled distance. The two monkeys with modest motor symptoms, as assessed with the Schneider score (Mk-LY and Mk-LL), exhibited quite a different decrease of striatal 18F-DOPA uptake, 17% and 84%, respectively. However, this high inter-individual difference, which was not reflected by the Schneider score, was consistent with the magnitude of increase of time spent in freezing state, which was more prominent in Mk-LL than in Mk-LY (Figure 3). Furthermore, spontaneous motion activity data in Mk-LL were not dramatically different from the other monkeys (Mk-MY and Mk-MI: Figure 3), which is consistent with the observation that all three monkeys exhibited a comparable striatal 18F-DOPA uptake drop following MPTP lesioning (Figure 4A). Although it has been reported that stable motor deficits occur in case of striatal dopaminergic depletion of at least 80% [51], a more reliable correlation between motor symptoms and dopaminergic depletion may require the acquisition of a vast palette of motor parameters in order to assess distinct motor attributes, which may be affected differently by graded dopaminergic depletions. The discrepancy observed in the present study between clinical score and spontaneous motion activity data appears in contradiction with a previous report [49] comparing these 2 parameters.

The small number of animals used (n=4) in order to meet ethical guidelines related to the use of non-human primates is a clear limitation of the present study. However, as illustrated in (Figures 3C and 3D), the focus here is more on an intra-individual comparison rather than a comparison with a control group. In other words, in the present study we compared in each individual monkey the post-MPTP phase exhibiting after one month a stable behavioral deficit, which is then partially reversed following the ANCE transplantation, thus providing evidence in favor of a positive impact of the cellular therapy. A further limitation is the variability of the MPTP model, as only one monkey (Mk-MI) exhibited post-lesion motor symptoms representing an optimal compromise between a behavioral state not too deleterious (e.g. self-feeding preserved) but still sufficiently diminished and stable in order to test the impact of ANCE transplantation-based therapy. To our knowledge, there is no report in the literature of such outstanding functional recovery as shown by Mk-MI (Movie 1), which could be attributed exclusively to spontaneous mechanisms. The evolution of the motor status of Mk-MI throughout the experiment, as illustrated in Movie 1, thus represents a strong additional case supporting the beneficial effect of ANCE transplantation, and confirming previous observations based on a larger group of monkeys [26,27]. The ANCE therapeutic approach has been shown, in the non-human primate as well, to be also promising in order to enhance the recovery from motor cortex lesion [37], leading to possible clinical applications in case of stroke for instance.

The transplantation of ANCE in a MPTP model comparable to ours previously showed an impressive cell survival rate reaching up to 50% at four months post-transplantation [26,27], contrasting with several embryonic and fetal transplantation studies reporting low cellular survival rates following transplantation [52-54]. Such large survival rate of ANCE may promote enough release of growth factors,

like GDNF and BDNF, which are known to be both present in in-vitro culture and in histological analyses, then possibly and indirectly being responsible for the enhanced behavioral recovery [26,27]. Taken together, the results of the present study support the hypothesis that the ANCE indirectly promotes neuroprotective and sprouting effects on the remaining dopaminergic system, as previously reported by Brunet and colleagues [27].

Over the last two decades, the potential of cell therapies as treatments for PD has been extensively investigated [55-61] with often disappointing results and limitations. By bypassing some ethical and immunological barriers, several studies reported both a neuroprotective and a restorative effect in PD animal model [61-63]. On a behavioral point of view, GDNF delivery was accompanied with a significant improvement of the parkinsonian symptoms in monkey MPTP models [55,57,61,64,65]. Importantly, for the first time, the protocols of ANCE production and culture were conducted in the present study under strict good manufacture practices (GMP) in a Swiss medic accredited facility. The GMP implementation represents a crucial and necessary step to move toward future clinical applications.

Conclusion

Using 18F-DOPA PET scan imaging the present research provides original evidence that the striatal dopaminergic activity can be recovered to a significant extent following autologous transplantation of adult neural progenitor cells, although the latter are not dopaminergic. On the clinical point of view, the final goal is to improve the neurological deficits, irrespective of whether there is a direct recovery of the dopaminergic system, via dopaminergic cells transplantation, or indirectly via another mechanism (other cell types promoting neurotrophic factors). The present PET data parallel significant functional motor recovery (assessed with spontaneous motion activity and Schneider scale). The presently observed improvement of motor symptoms confirms previously reported proof of principle for such autologous cell therapy [26] in MPTP-intoxicated monkeys.

Acknowledgement

Cell culture: Dr. Laurent Waselle, Isabelle Sénéchaud, Florence Dubugnon-Dauman, Gilles Goumaz.

PET facility at HFR: Didier Maillard, Bernard Gex.

LI-COR bioscience analysis: Prof. Zhihong Yang, Dr. Yuyan Xiong.

Animal care takers: Laurent Bossy and Jacques Maillard.

Mechanic and electronic workshop: André Gaillard, Andrea Francovich, Bernard Aebischer.

Informatics: Laurent Monney

Funding

Swiss National Science Foundation (SNF), Grant Nos 31-61857.00, 310000-110005, 31003A-132465 and 31003A-149643 (EMR), No 3100A0-103924 (JB), Sinergia project PROMETHEUS CRSI33_125408; the Swiss Primate Competence Centre for Research (SPCCR).

Movie 1: Four time periods illustrating qualitatively the general motor behavior. The first time window shows how intact monkeys behave in the detention room, exhibiting normal motor patterns. The next three sequences illustrate the specific motor behavior of Mk-MI at three time points: i) 4 days post-MPTP lesion; ii) 3 weeks post-MPTP lesion; iii) three months post-ANCE transplantation.

The video sequence is available at:

http://www.unifr.ch/neuro/rouiller/research/own-projects/motor/parkinson/mptp

Movie 2: The video sequence illustrates the test of spontaneous motion activity and typical data obtained for Mk-MI.

The video sequence is available at:

http://www.unifr.ch/neuro/rouiller/research/own-projects/motor/parkinson/mptp

References

1. Lang AE, Lozano AM (1998) Parkinson's disease. First of two parts. N Engl J Med 339: 1044-1053.
2. Dauer W, Przedborski S (2003) Parkinson's disease: Mechanisms and models. Neuron 39: 889-909.
3. Schulz JB, Falkenburger BH (2004) Neuronal pathology in Parkinson's disease. Cell Tissue Res 318: 135-147.
4. Hornykiewicz O (2006) The discovery of dopamine deficiency in the Parkinsonian brain. J Neural Transm Suppl 70: 9-15.
5. Jankovic J (2008) Parkinson's disease: Clinical features and diagnosis. J Neurol Neurosurg Psychiatry 79: 368-376.
6. Hirsch EC, Jenner P, Przedborski S (2013) Pathogenesis of Parkinson's disease. Mov Disord 28: 24-30.
7. Vingerhoets FJG, Schulzer M, Calne DB, Snow BJ (1997) Which clinical sign of Parkinson's disease best reflects the nigrostriatal lesion? Ann Neurol 41: 58-64.
8. Pate BD, Kawamata T, Yamada T, McGeer EG, Hewitt KA, et al. (1993) Correlation of striatal fluorodopa uptake in the MPTP monkey with dopaminergic indices. Ann Neurol 34: 331-338.
9. Doudet DJ, Miyake H, Finn RT, McLellan CA, Aigner TG, et al. (1989) 6-18F-L-dopa imaging of the dopamine neostriatal system in normal and clinically normal MPTP-treated rhesus monkeys. Exp Brain Res 78: 69-80.
10. Snow BJ, Tooyama I, McGeer EG, Yamada T, Calne DB, et al. (1993) Human positron emission tomographic [18F] fluorodopa studies correlate with dopamine cell counts and levels. Ann Neurol 34: 324-330.
11. Blesa J, Pifl C, Sánchez-González MA, Juri C, García-Cabezas MA, et al. (2012) The nigrostriatal system in the presymptomatic and symptomatic stages in the MPTP monkey model: A PET, histological and biochemical study. Neurobiol Dis 48: 79-91.
12. Schrag A, Quinn N (2000) Dyskinesias and motor fluctuations in Parkinson's diseaseA community-based study. Brain 123: 2297-2305.
13. Benabid AL (2003) Deep brain stimulation for Parkinson's disease. Curr Opin Neurobiol 13: 696-706.
14. Benabid AL, Chabardes S, Mitrofanis J, Pollak P (2009) Deep brain stimulation of the subthalamic nucleus for the treatment of Parkinson's disease. Lancet Neurol 8: 67-81.
15. Bronstein JM, Tagliati M, Alterman RL, Lozano AM, Volkmann J, et al. (2011) Deep brain stimulation for Parkinson disease: An expert consensus and review of key issues. Arch. Neurol 68: 165.
16. Williams NR, Okun MS (2013) Deep brain stimulation (DBS) at the interface of neurology and psychiatry. J Clin Invest 123: 4546-4556.
17. Morizane A, Li JY, Brundin P (2008) From bench to bed: the potential of stem cells for the treatment of Parkinson's disease. Cell Tissue Res 331: 323-336.
18. Freed CR, Greene PE, Breeze RE, Tsai WY, DuMouchel W, et al. (2001) Transplantation of embryonic dopamine neurons for severe Parkinson's disease. N Engl J Med 344: 710-719.
19. Olanow CW, Goetz CG, Kordower JH, Stoessl AJ, Sossi V, et al. (2003) A double-blind controlled trial of bilateral fetal nigral transplantation in Parkinson's disease. Ann Neurol 54: 403-414.
20. Brederlau A, Correia AS, Anisimov SV, Elmi M, Paul G, et al. (2006) Transplantation of human embryonic stem cell-derived cells to a rat model of Parkinson's disease: Effect of *in vitro* differentiation on graft survival and teratoma formation. Stem Cells 24: 1433-1440.
21. Lee AS, Tang C, Cao F, Xie X, van der Bogt K, et al. (2009) Effects of cell number on teratoma formation by human embryonic stem cells. Cell Cycle 8: 2608-2612.
22. Hallett PJ, Deleidi M, Astradsson A, et al. (2015) Successful function of autologous iPSC-derived dopamine neurons following transplantation in a non-human primate model of Parkinson's disease. Cell Stem Cell 16: 269-274.

23. Brunet J-F, Pellerin L, Arsenijevic Y, Magistretti P, Villemure JG (2002) A novel method for in vitro production of human glial-like cells from neurosurgical resection tissue. Lab. Invest 82: 809-812.

24. Brunet JF, Rouiller E, Wannier T, Villemure JG, Bloch J (2005) Primate adult brain cell autotransplantation, a new tool for brain repair? Exp Neurol 196: 195-198.

25. Bloch J, Kaeser M, Sadeghi Y, Rouiller EM, Redmond DE Jr, et al. (2011) Doublecortin-positive cells in the adult primate cerebral cortex and possible role in brain plasticity and development. J Comp Neurol 519: 775-789.

26. Bloch J, Brunet JF, McEntire CRS, Redmond DE (2014) Primate adult brain cell autotransplantation produces behavioral and biological recovery in 1-methyl-4-phenyl-1,2,3,6-tetrahydropyridine-induced parkinsonian St. Kitts monkeys. J Comp Neurol 522: 2729-2740.

27. Brunet JF, Redmond DE Jr, Bloch J (2009) Primate adult brain cell autotransplantation: A pilot study in asymptomatic MPTP-treated monkeys. Cell Transplant 18: 787-799.

28. Chassain C, Eschalier A, Durif F (2001) Assessment of motor behavior using a video system and a clinical rating scale in Parkinsonian monkeys lesioned by MPTP. J Neurosci Methods 111: 9-16.

29. Badoud S, Borgognon S, Cottet J, Chatagny P, Moret V, et al. (2017) Effects of dorsolateral prefrontal cortex lesion on motor habit and performance assessed with manual grasping and control of force in macaque monkeys. Brain Struct Funct 222: 1193-1206.

30. Schneider JS, Lidsky TI, Hawks T, Mazziotta JC, Hoffman JM (1995) Differential recovery of volitional motor function, lateralized cognitive function, dopamine agonist-induced rotation and dopaminergic parameters in monkeys made hemi-Parkinsonian by intracarotid MPTP infusion. Brain Res 672: 112-127.

31. Whone AL, Bailey DL, Remy P, Pavese N, Brooks D (2004) A technique for standardized central analysis of 6-18F-Fluoro-l-DOPA PET data from a multicenter study. J Nucl Med 45: 1135-1145.

32. Collantes M, Prieto E, Peñuelas I, Blesa J, Juri C, et al. (2009) New MRI, 18F-DOPA and 11C-(+)-alpha-dihydrotetrabenazine templates for *Macaca fascicularis* neuroimaging: Advantages to improve PET quantification. Neuroimage 47: 533-539.

33. Patlak CS, Blasberg RG (1985) Graphical evaluation of blood-to-brain transfer constants from multiple-time uptake data. Generalizations. J Cereb Blood Flow Metab 5: 584-590.

34. Mounayar S, Boulet S, Tande D, Jan C, Pessiglione M, et al. (2007) A new model to study compensatory mechanisms in MPTP-treated monkeys exhibiting recovery. Brain 130: 2898-2914.

35. Kaeser M, Wannier T, Brunet JF, Wyss A, Bloch J, et al. (2013) Representation of motor habit in a sequence of repetitive reach and grasp movements performed by macaque monkeys: Evidence for a contribution of the dorsolateral prefrontal cortex. Cortex 49: 1404-1419.

36. Brunet JF, Pellerin L, Magistretti P, Villemure JG (2003) Cryopreservation of human brain tissue allowing timely production of viable adult human brain cells for autologous transplantation. Cryobiology 47: 179-183.

37. Kaeser M, Brunet JF, Wyss A, Belhaj-Saif A, Liu Y, et al. (2011) Autologous adult cortical cell transplantation enhances functional recovery following unilateral lesion of motor cortex in primates: A pilot study. Neurosurgery 68: 1416-1417.

38. Paxinos G, Huang X, Toga AW (1999) The rhesus monkey brain in stereotaxic coordinates. San Diego, USA: Academic Press.

39. Melega WP, Hoffman JM, Schneider JS, Phelps ME, Barrio JR, et al. (1991) 6-[18F] fluoro-L-dopa metabolism in MPTP-treated monkeys: assessment of tracer methodologies for positron emission tomography. Brain Res 543: 271-276.

40. Melega WP, Raleigh MJ, Stout DB, DeSalles AA, Cherry SR, et al. (1996) Longitudinal behavioral and 6-[18F]Fluoro-l-DOPA-PET assessment in MPTP-Hemiparkinsonian monkeys. Exp Neurol 141: 318-329.

41. Blesa J, Juri C, Collantes M, Peñuelas I, Prieto E, et al. (2010) Progression of dopaminergic depletion in a model of MPTP-induced Parkinsonism in non-human primates. An 18F-DOPA and 11C-DTBZ PET study. Neurobiol Dis 38: 456-463.

42. Liu Y, Yue F, Tang R, Tao G, Pan X, et al. (2014) Progressive loss of striatal dopamine terminals in MPTP-induced acute parkinsonism in cynomolgus monkeys using vesicular monoamine transporter type 2 PET imaging ([18F] AV-133). Neurosci Bull 30: 409-416.

43. Song DD, Haber SN (2000) Striatal responses to partial dopaminergic lesion: Evidence for compensatory sprouting. J Neurosci 20: 5102-5114.

44. Boulet S, Mounayar S, Poupard A, Bertrand A, Jan C, et al. (2008) Behavioral recovery in MPTP-treated monkeys: Neurochemical mechanisms studied by intrastriatal microdialysis. J Neurosci 28: 9575-9584.

45. Ballanger B, Beaudoin-Gobert M, Neumane S, Epinat J, Metereau E, et al. (2016) Imaging dopamine and serotonin systems on MPTP monkeys: A longitudinal pet investigation of compensatory mechanisms. J Neurosci 36: 1577-1589.

46. Potts LF, Wu H, Singh A, Marcilla I, Luquin MR, et al. (2014) Modeling Parkinson's disease in monkeys for translational studies, a critical analysis. Exp Neurol 256: 133-143.

47. Eidelberg E, Brooks BA, Morgan WW, Walden JG, Kokemoor RH (1986) Variability and functional recovery in the N-methyl-4-phenyl-1,2,3,6-tetrahydropyridine model of Parkinsonism in monkeys. Neurosci 18: 817-822.

48. Collier TJ, Steece-Collier K, Kordower JH (2003) Primate models of Parkinson's disease. Exp Neurol 183: 258-262.

49. Liu N, Yue F, Tang WP, Chan P (2009) An objective measurement of locomotion behavior for hemiparkinsonian cynomolgus monkeys. J Neurosci Methods 183: 188-194.

50. Worbe Y, Baup N, Grabli D, Chaigneau M, Mounayar S, et al. (2009) Behavioral and movement disorders induced by local inhibitory dysfunction in primate striatum. Cerebral Cortex 19: 1844-1856.

51. Soderstrom K, O'Malley J, Steece-Collier K, Kordower JH (2006) Neural repair strategies for Parkinson's disease: Insights from primate models. Cell Transplant 15: 251-265.

52. Brundin P, Björklund A (1987) Survival, growth and function of dopaminergic neurons grafted to the brain. Prog Brain Res 71: 293-308.

53. Brundin P, Karlsson J, Emgård M, Schierle GS, Hansson O, et al. (2000) Improving the survival of grafted dopaminergic neurons: A review over current approaches. Cell Transplant 9: 179-195.

54. Hagell P, Brundin P (2001) Cell survival and clinical outcome following intrastriatal transplantation in Parkinson disease. J Neuropathol Exp Neurol 60: 741-752.

55. Gash DM, Zhang Z, Ovadia A, Cass WA, Yi A, et al. (1996) Functional recovery in Parkinsonian monkeys treated with GDNF. Nature 380: 252-255.

56. Choi-Lundberg DL, Lin Q, Chang YN, Chiang YL, Hay CM, et al. (1997) Dopaminergic neurons protected from degeneration by GDNF gene therapy. Science 275: 838-841.

57. Kordower JH, Emborg ME, Bloch J, Ma SY, Chu Y, et al. (2000) Neurodegeneration prevented by lentiviral vector delivery of GDNF in primate models of Parkinson's disease. Science 290: 767-773.

58. Patel NK, Bunnage M, Plaha P, Svendsen CN, Heywood P, et al. (2005) Intraputamenal infusion of glial cell line-derived neurotrophic factor in PD: A two year outcome study. Ann Neurol 57: 298-302.

59. Slevin JT, Gerhardt GA, Smith CD, Gash DM, Kryscio R, et al. (2005) Improvement of bilateral motor functions in patients with Parkinson disease through the unilateral intraputaminal infusion of glial cell line-derived neurotrophic factor. J Neurosurg 102: 216-222.

60. Lang AE, Gill S, Patel NK, Lozano A, Nutt JG, et al. (2006) Randomized controlled trial of intraputamenal glial cell line–derived neurotrophic factor infusion in Parkinson disease. Ann Neurol 59: 459-466.

61. Ren Z, Wang J, Wang S, Zou C, Li X, et al. (2012) Autologous transplantation of GDNF-expressing mesenchymal stem cells protects against MPTP-induced damage in cynomolgus monkeys. Sci Rep 3: 2786.

62. Tomac A, Lindqvist E, Lin LF, Ogren SO, Young D, et al. (1995) Protection and repair of the nigrostriatal dopaminergic system by GDNF *in vivo*. Nature 373: 335-339.

63. Sinclair SR, Svendsen CN, Torres EM, Martin D, Fawcett JW, et al. (1996) GDNF enhances dopaminergic cell survival and fibre outgrowth in embryonic nigral grafts. Neuroreport 7: 2547-2552.

64. Emborg ME, Ebert AD, Moirano J, Peng S, Suzuki M, et al. (2018) GDNF-secreting human neural progenitor cells increase tyrosine hydroxylase and VMAT2 expression in MPTP-treated cynomolgus monkeys. Cell Transplant 17: 383-395.

65. Redmond DE Jr, Elsworth JD, Roth RH, Leranth C, Collier TJ, et al. (2009) Embryonic substantia nigra grafts in the mesencephalon send neurites to the host striatum in non-human primate after overexpression of GDNF. J Comp Neurol 515: 31-40.

Citation: Borgognon S, Cottet J, Moret V, Chatagny P, Ginovart N, et al. (2017) Enhancement of Striatal Dopaminergic Function Following Autologous Neural Cell Ecosystems (ANCE) Transplantation in a Non-Human Primate Model of Parkinson's Disease. J Alzheimers Dis Parkinsonism 7: 383. doi: 10.4172/2161-0460.1000383